# Activation of NRF2/FPN1 Pathway Attenuates Myocardial Ischemia-reperfusion Injury in Diabetic Rats by Regulating Iron Homeostasis and Ferroptosis

**hao tian**
Renmin Hospital of Wuhan University: Wuhan University Renmin Hospital
**Yonghong Xiong**
Renmin Hospital of Wuhan University: Wuhan University Renmin Hospital
**Yi Zhang**
Shandong Qianfoshan Hospital
**Yan Leng**
Renmin Hospital of Wuhan University: Wuhan University Renmin Hospital
**Jie Tao**
Renmin Hospital of Wuhan University: Wuhan University Renmin Hospital
**Lu Li**
Renmin Hospital of Wuhan University: Wuhan University Renmin Hospital
**Zhen Qiu**
Renmin Hospital of Wuhan University: Wuhan University Renmin Hospital
**Zhongyuan Xia** ( xiazhongyuan2005@aliyun.com )
Renmin Hospital of Wuhan University: Wuhan University Renmin Hospital https://orcid.org/0000-0002-5807-9554

**Research Article**

**Keywords:** nuclear factor E2-related factor 2, ferroportin1, iron homeostasis, ferroptosis, diabetes, myocardial ischemia-reperfusion injury

**Posted Date:** November 11th, 2021

**DOI:** https://doi.org/10.21203/rs.3.rs-1041842/v1

**Version of Record:** A version of this preprint was published at Cell Stress and Chaperones on February 5th, 2022. See the published version at https://doi.org/10.1007/s12192-022-01257-1.

# Abstract

**Purpose** Myocardial ischemia-reperfusion injury (IRI) can further worsen cardiac function in ischemic heart disease, and diabetes can increase susceptibility to myocardial IRI. Disorders of iron metabolism are involved in the pathological mechanisms of the most common diseases, such as diabetes, obesity, coronary artery angioplasty, or heart transplantation. Ferroportin1 (FPN1) is the only protein known to be associated with iron release in mammals and is regulated by nuclear factor E2-related factor 2 (NRF2) at the transcriptional level, thus playing an important role in iron homeostasis. Therefore, this study tested whether NRF2/FPN1 pathway plays a beneficial role in the treatment of diabetic myocardial IRI and potential detailed mechanism.

**Methods** In this study, we investigated the effects of ferroptosis in STZ-induced diabetic rats following myocardial IRI in vivo, and its alteration in glucose and hypoxia/reoxygenation-induced cardiomyocytes injury in vitro.

**Results** Cardiac functional and structural damage was detected by Evans blue/TTC double staining, Echocardiography, HE staining and serological indices, CCK-8 assay and ROS production to measure cardiomyocyte viability and oxidative stress level. Additionally, the changes in cell supernatant levels of $Fe^{2+}$, SOD, MDA, and mRNA and protein expression of ferroptosis marker proteins confirmed the beneficial effects of the NRF2/FPN1 pathway on diabetic myocardial IRI related to iron metabolism and ferroptosis.

**Conclusions** Overall, we find that iron homeostasis-related ferroptosis plays an important role in aggravating myocardial IRI in diabetic rats, and NRF2/FPN1 pathway-mediated iron homeostasis and ferroptosis might be a promising therapeutic target against myocardial IRI in diabetes.


# Introduction

Diabetes is a chronic metabolic disease characterized by high glucose, and its prevalence and disability rates have exploded in recent years. The long-standing hyperglycemia state can cause chronic damage and dysfunction of various tissues, especially the heart and blood vessels. Ischemic heart disease, especially acute myocardial infarction, is a fatal threat to diabetic patients. In order to save the ischemic myocardium, coronary blood flow must be re-established. However, during this process, sometimes there could be aggravated structural and functional damage, known as ischemia-reperfusion injury (IRI)[1]. According to previous researches, diabetes can exacerbate myocardial IRI by producing oxidative stress through related pathways which activated the occurrence of apoptosis, inflammation, autophagy, and so on[2–4]. However, the main related mechanisms of myocardial IRI in diabetes need to be further clarified.

Ferroptosis is a recently recognized form of iron-dependent programmed cell death that based on the inactivation of the lipid repair enzyme glutathione peroxidase 4 (GPX4) and subsequent accumulation of reactive oxygen species (ROS) in lipids. Studies have shown that iron chelators, such as desferrioxamine, could significantly inhibit Erastin-induced cellular ferroptosis. This suggests that iron homeostasis plays

a key role in the onset of cellular ferroptosis[5]. Other studies have shown that cell membranes and plasma membranes containing polyunsaturated fatty acids are particularly susceptible to peroxidation with lipid radicals, and the rate of this reaction is greatly increased in the presence of iron[6]. Thus, irons are essential components for lipid peroxide accumulation and initiation of the ferroptosis process.

Iron is an indispensable trace metal element in many physiological activities. Its homeostatic balances are regulated precisely in internal bodies, because no matter excess or deficiency of iron are potential risk factors. Imbalances in iron homeostasis have been reported to be involved in a variety of diseases such as cancer, anemia, neurodegenerative diseases, and heart disease [7]. Iron uptake and iron release are key steps in the regulation of cellular iron metabolism. Cardiomyocytes possess multiple iron input systems. Ferroportin1 (FPN1) is the only iron release related protein known in mammals and plays an important role in iron homeostasis at the systemic level. It is a transmembrane protein encoded by the SLC40A1 gene and is responsible for exporting iron from the cell to the plasma [8]. Studies have shown that FPN1 is involved in maintaining iron homeostasis in cardiomyocytes under conditions of iron deficiency or iron overload [9]. In addition, nuclear factor E2-related factor 2 (NRF2) regulates FPN1 expression at the transcriptional level [10].

Human NRF2, known as a critical regulator of the antioxidant response, is a transcription factor encoded by the NFE2L2 gene and belongs to the leucine zipper structure family[11]. Oxidative stress plays an important role in the process of diabetes and its complications [12]. And oxidative stress is considered as one of the main causes of cardiac dysfunction during myocardial ischemia-reperfusion[13]. Zhang et al have demonstrated that myocardial oxidative damage and cell death could be ameliorated by activating NRF2-associated signaling pathways, and thus the myocardial IRI of T1D was alleviated[14]. Other studies showed that the expression of FPN1 was decreased in NRF2 knockout mice[15]. Furthermore, studies have found that myocardium can be protected from ferroptosis by regulating NRF2 expression [16, 17]. However, the NRF2-FPN1 interaction relationship in diabetic myocardial IRI has not been reported. Therefore, the purpose of our present study aims to test the hypotheses that NRF2/FPN1 signaling pathway-mediated iron homeostasis and ferroptosis play a crucial role in diabetic myocardial IRI, which may be a protective mechanism against diabetic myocardial IRI.

# Materials And Methods

### Animals and Diabetes Induction

The animal experimental protocol was approved by the Bioethics Committee of Renmin Hospital of Wuhan University. Healthy male adult Sprague-Dawley (SD) rats were supplied by Beijing Vital River Bioscience Co. Ltd, weighing 200-220g, 6-8weeks old. After 5 days of acclimatization, the rats were fasted for 12 h for diabetes induction. The diabetic rats were administered a single intraperitoneal injection of 60 mg/kg streptozotocin (STZ) dissolved in citrate buffer to induce diabetes as described previously[18]. The non-diabetic rats were injected with an equal volume of sodium citrate buffer. After 72h (with 6h

fasting), the rats exhibiting hyperglycemia (blood glucose level higher than 16.7 mmol/l), polyphagia, polydipsia and polyuria were considered to have diabetes.

## Reagents

Streptozotocin (STZ), triphenyl tetrazolium chloride (TTC) and Evans blue (EB) were purchased from Sigma Chemical Co. (MO, USA). Dulbecco's modified Eagle's medium (DMEM) and fetal bovine serum (FBS) were obtained from Gibco Laboratories (Grand Island, NY, USA). Sulforaphane (SFN), the NRF2 agonist was purchased from Glpbio Co. (CA, USA). Erastin (Era), the ferroptosis agonist was purchased from Selleck (Houston, TX).The cell counting kit-8 (CCK-8) and 2',7'-dichlorofluorescein diacetate (DCFH-DA) assay test kits were obtained from Beyotime Institute of Biotechnology (Shanghai, China). Lactate dehydrogenase (LDH), enzyme-linked immunosorbent assay (ELISA),superoxide dismutase (SOD), malondialdehyde (MDA) and $Fe^{2+}$ assay test kits were purchased from Nanjing Jiancheng Bioengineering Institute (Nanjing, Jiangsu, China). The primers for NRF2, FPN1, ACSL4 and β-actin were designed and synthesized by Wuhan servicebio Co. (Wuhan, Hubei, China). NRF2 primary antibodies were purchased from Cell Signaling Technology (CST, Beverly, CA, USA). FPN1, ACSL4, GPX4 and GAPDH primary antibodies were obtained from Proteintech Co. (Wuhan, Hubei, China).

## Glucose tolerance Testing

The diabetic rats fasted overnight, and then glucose was administered at a dose of 2g/kg by gastric lavage or intraperitoneally injection to conduct the oral glucose tolerance test (OGTT) and intraperitoneal glucose tolerance test (IPGTT) to confirm the success of animal model. Blood glucose level was measured at 0 (before glucose load), 30, 60, 90, and 120 min. All blood samples were collected from the tail to determine plasma glucose.

## Myocardial Ischemia and Reperfusion Model

Rats were anesthetized by intraperitoneal injection of 1% sodium pentobarbital (60mg/kg) and managed for electrocardiogram (ECG) monitoring. After disinfection of skin, tracheotomy was performed and the ventilator was connected for mechanical ventilation. The ribs were cut at the 3rd to 4th intercostal space in the left midclavicular line and the entire heart is fully exposed. Subsequently, the left anterior descending coronary artery (LAD) below the left auricle was ligated with a 7-0 silk wire. Successful ischemia is indicated when there is a change in color from red to white in the apical region and left ventricular wall with reduced ventricular wall motion and an elevated ST-segment arch in the ECG. After 30 min, the apical and left ventricular color gradually returned to red and the ST-segment recovered, suggesting successful reperfusion, as seen by loosening the ligature.Lastly, the myocardium was reperfused for 2h (for protein expression and serological indicators measurement) or 72h (for cardiac function measurement). Furthermore, the ligation thread was passed through the LAD but not ligated in the sham operation group.

## Experimental Protocols

For the in vivo study, 8 weeks after STZ injection, all rats were randomly divided into 4 groups: (1) normal + sham group (NS); (2) normal + ischemia-reperfusion group (NIR); (3) diabetes + sham group (DS); (4) diabetes + ischemia-reperfusion group (DIR).To gain a deeper insight into the effect of NRF2 activation, the following expriments were preformed among diabetic rats: (1) diabetes + ischemia-reperfusion group (DIR); (2) diabetes + ischemia-reperfusion + sulforaphane group (DIR + SFN); (3) diabetes + ischemia-reperfusion + SFN+Erastin group (DIR + SFN + Era). Each group contains 8 rats. The NRF2 agonist sulforaphane (500mg/kg/day) was injected intraperitoneally for 3 days before ischemia[19]. And the ferroptosis agonist Erastin (20mg/kg) was injected intraperitoneally at the beginning of the ischemia-reperfusion operation.

For the in vitro study, H9c2 cardiomyocytes were randomly assigned to 6 groups: (1) low glucose group (5.5 mM); (2) low glucose + hypoxia-reoxygenation group (H/R) ; (3) high glucose group (HG) (30mM); (4) high glucose + hypoxia-reoxygenation group (HH/R); (5) high glucose + hypoxia-reoxygenation + sulforaphane group (HH/R + SFN); (6) high glucose + hypoxia-reoxygenation + sulforaphane + Erastin group (HH/R + SFN + Era). H9c2 cardiomyocytes of all groups were cultured in low-glucose DMEM containing 10% FBS and 1% penicillin/streptomycin and incubated in normoxic incubator at 37℃ in a humidified atmosphere of 5% $CO_2$. When the density of H9c2 cardiomyocytes reached 70%-80%, all cells were digested with trypsin containing ethylenediaminetetraacetic acid (EDTA) and transferred to 6-well culture plates for subsequent experimental treatments. To simulate the high glycemic state，cells were cultured in serum-free medium overnight and exposed to HG medium for 24 h. For the H/R cell model, cells were subjected to hypoxic state (94% $N_2$ + 5% $CO_2$ + 1% $O_2$) for 6h and followed by reoxygenation (95% air + 5% $CO_2$) for 2h. Sulforaphane and Erastin was given 24h before H/R. The experimental protocol is depicted schematically in Fig. 1.

## Determination of Myocardial Infarction

After 2h of ischemia-reperfusion treatment, six rats in each group were randomly selected to ligate LAD along with the original site. The 2% Evans Blue reagent was slowly injected from the femoral vein, while the non-ischemic area showed blue staining region.The aorta was immediately clamped and the heart was removed and sliced along the longitudinal axis. Five pieces of heart slices were prepared, placed in the 1% TTC solution in a 37℃ incubator for 30 min in the dark. The slices were then fixed in 4% paraformaldehyde for 30 min, scanned by the scanner (Epson, v30, Japan). And the myocardium area was calculated with an image analysis system (Image J; National Institutes of Health, USA). Theoretically, normal myocardium appears blue, ischemic myocardium shows brick-red, and infarcted myocardium displays pale. For ischemic myocardium stained by TTC staining, brick-red myocardium was defined as the area at risk (AAR) and pale myocardium was defined as the infarct area (IA). The percentage of myocardial infarction area was calculated as IA versus AAR (IA/AAR×100%).

## Echocardiography

In order to avoid the interference of residual gas in the thoracic cavity on the echocardiography after thoracotomy, 6 rats were taken from each group after 72h of reperfusion. Rats were anesthetized with 2-3% inhaled isoflurane and fixed on the operating table.The MyLab 30CV ultrasound system (Biosound Esaote, Indianapolis, IN, USA) with a 15-MHz transducer probe was used to perform two-dimensional and M-mode echocardiographic measurements. Parasternal long axis and short axis images were obtained in short and long axes in two-dimensional and M-mode for quantification. Left ventricular internal dimension systole (LVIDs) and left ventricular internal dimension diastole (LVIDd) were measured on the parasternal LV long axis view. Left ventricular ejection fraction (LVEF) and left ventricular shortening fraction (LVFS) were calculated by computer algorithms. All measurements that represented the mean of 5 consecutive cardiac cycles, were performed in a blinded manner.

### Hematoxylin and eosin staining

Myocardial tissue was fixed overnight in 4% paraformaldehyde at 4°C. The tissue was then dehydrated in a series of ethanol and xylene solutions and embedded in paraffin wax. Cut the heart tissue block into 4μm thick tissue sections with a microtome. According to the manufacturer's instructions, hematoxylin and eosin (HE) staining was performed to assess the morphological changes and damage degree.

### Measurement of serum CK-MB and LDH levels

At the end of reperfusion, arterial blood samples were collected and centrifuged at 1200 rpm for 15 min. The creatine kinase-MB (CK-MB) was detected by an ELISA kit and lactate dehydrogenase (LDH) was detected by colorimetry with an LDH assay kit according to the manufacturer's instructions.

### Cell Viability Assay

Cells were plated in 96-well plates at a density of 3000 cells/well, grouped according to the experiment (5 replicate wells per group). After cells were cultured and treated in 96-well plates, 10 μL of CCK-8 reagent was added to each well and then incubated for 2 hours in the dark. Absorbance was detected at 450 nm with a microplate reader (Perkin Elmer, USA).

### Measurement of malondialdehyde (MDA) level, ferrous ion ($Fe^{2+}$) level, superoxide dismutase (SOD) activity

After modeling, the cells and cell supernatant were collected to measure the malondialdehyde (MDA) level, antioxidant enzyme superoxide dismutase (SOD) activity and intracellular $Fe^{2+}$ concentration by spectrophotometry according to the manufacturer’s instructions. Then, the intensity was observed by a microplate reader.

### ROS measurement

Intracellular reactive oxygen levels were measured with the 2',7'-dichlorofluorescein diacetate (DCFH-DA) molecular probe. Briefly, cardiomyocytes in 6-well plates were loaded with the appropriate amount of

DCFH-DA probe for 30 min at 37°C in the dark. DCFH-DA was oxidized and converted to highly fluorescent DCFH and showed green fluorescence in the cytoplasmic lysate. Fluorescence images were captured by a fluorescence microscope (Olympus, Tokyo, Japan).

### Immunofluorescence

H9c2 cardiomyocytes in 6-well plates were fixed with 4 % paraformaldehyde for 30 min. After that, they were permeabilized in 0.5 % Triton X-100 at 37°C for 20 min, blocked with 5% BSA solution and add NRF2 antibody to incubate overnight at 4°C. Finally, the samples were incubated with Cy3 labeled goat anti-rabbit secondary antibody, followed by 4',6-diamidino-2-phenylindole dihydrochloride (DAPI) (Invitrogen, Carlsbad, CA, USA) staining for 10min, then observed and captured positive areas with a laser confocal microscope (Leica TCS, Germany).

### Quantitative real-time polymerase chain reaction (qRT-PCR) analysis

Total RNA was extracted from the myocardial samples and H9c2 cells using Trizol reagent. 2 μg of RNA from each sample was then reverse transcribed into cDNA according to the Prime-Script RT reagent kit instruction(Servicebio, Wuhan, Hubei, China). The qRT-PCR was performed using a SYBR Green qPCR Reagent Kit (Servicebio, Wuhan, Hubei, China) by Bio-Rad CFX Connect Real-Time PCR Detection System (Bio-Rad, USA). The primers used are listed in Table 1. The mRNA levels were normalized to β-actin mRNA level. The expression of genes was analysed by using the $2^{-\Delta\Delta CT}$ method.

Table 1. The sequences of RT-PCR used in this study

| Gene | Forward (5'-3') | Reverse (5'-3') |
|---|---|---|
| ACSL4 | CTGCCGAGTGAATAACTTTGGA | TCAGATAGGAAGCCTCAGACTCATT |
| NRF2 | TTGGGGTAAGTCGAGAAGTGTTT | ATGTGGGCAACCTGGGAGTA |
| SLC40A1 | CTAAATCCGTCCCCATAATCTCC | CCCATTGCCACAAAGGAGAC |
| β-actin | TGCTATGTTGCCCTAGACTTCG | GTTGGCATAGAGGTCTTTACGG |

### Western blotting

After different treatments, H9c2 cardiomyocytes and myocardial tissue were homogenized with pre-cooled RIPA lysis buffer. The supernatant was taken and added to the protein buffer. Then, the extracts were placed at 100°C and keep them for 5 min. The total protein was separated by SDS-PAGE gel and then transferred to PVDF membranes. The membranes were incubated with 5% skimmed milk for 1 hour. Primary antibodies (ACSL4, 1:1000; GPX4, 1:1000; NRF2, 1:1000; FPN1, 1:1000; GAPDH, 1:1000) were incubated with the membranes overnight at 4°C. The horseradish peroxidase (HRP) conjugated secondary antibody (1:5000; Proteintech) was incubated for 1 h at room temperature. The final analysis was performed with the biological image analysis system (Bio-Rad, USA). The relative expression levels of the target proteins in each sample were obtained by normalizing these levels against that of GAPDH.

### Statistical analysis

All results were analyzed using Graphpad Prism 8.0 software (GraphPad Software, USA) and presented as means ± standard deviation. Statistical analysis was carried out using one-way analysis of variance (ANOVA) and $P < 0.05$ were deemed significant.

# Results

### The exacerbated myocardial IRI in diabetic rats was associated with the activation of ferroptosis and the downregulation of the NRF2/FPN1 pathway

After STZ induced diabetes, the diabetic rats showed characteristic symptoms of diabetes including hyperglycemia, polydipsia, polyphagia and weight reduction (Fig. 2A). Moreover, STZ induced rats exhibited markedly impaired IPGTT and OGTT (Fig. 2B). Therefore these data demonstrated that our diabetic animal models were successfully developed.

Ischemia-reperfusion significantly impaired cardiac function by decreasing LVEF and LVFS in both diabetic and non-diabetic animals. However, compared with the NIR group, DIR group showed further impaired cardiac function (Fig. 2C). Uniformly, compared with the NIR group, the diabetes markedly increased myocardial infarction area after ischemia-reperfusion treatment (Fig. 2D). In addition, compared with normal rats, diabetic rats had higher levels of LDH and CK-MB (Fig. 2E). HE staining showed that the structure of myocardial tissue in NS group remained clear, the cardiomyocytes were arranged neatly, and no fibrosis fraction were observed. The myocardial tissue in DS and NIR groups showed mild disorder of cell arrangement and a few myocardial fiber breakage. In the DIR group, the myocardial tissue showed severe cell alignment disorder, cell swelling and necrosis, and most of the myocardial fibers were tremendously broken (Fig. 2F). The above results indicated that the myocardial IRI was significantly exacerbated in diabetic rats compared with non-diabetic rats.

The NRF2 has been widely reported to play a novel role in diabetic myocardial IRI and also participates in ferroptosis[20, 21]. Meanwhile, some studies proved that at the transcriptional level, NRF2 can regulate the expression of FPN1, a protein that plays an important role in iron homeostasis at the systemic level and is currently the only known iron release related protein in mammals[22, 23]. Next, to determine the level of transcription in cardiomyocytes NRF2 and FPN1, we assessed the mRNA in cardiomyocytes in each group. Our experiments found that compared with the NS group, the protein and mRNA expression of NRF2 and FPN1 in DS and NIR group was lower (Fig. 2G-H). And it's not difficult to observe the mRNA and protein expression levels of NRF2 and FPN1 were significantly reduced in the DIR group. To date, both ACSL4 and GPX4 were well recognized biomarkers for ferroptosis. Western blot showed that compared with the NS group, the expression of ACSL4 in the DS group and the NIR group increased, and the expression of ACSL4 in the DIR group further increased (Fig. 2G). However, the level of GPX4 was opposite to ACSL4. And the expression level of mRNA of ACSL4 is consistent with protein (Fig. 2H). These data indicated that following myocardial ischemia-reperfusion treatment, impairment of the

NRF2/FPN1 signaling pathway causes development of ferroptosis to exacerbate the myocardial IRI, in diabetic rats compared with that in non-diabetic rats.

### The ferroptosis agonist could abrogate the protective effect of NRF2 agonist SFN in diabetic rats following myocardial IRI

To verify the contribution of NRF2/FPN1-dependent ferroptosis to diabetic myocardial IRI, the NRF2 agonist SFN was applied to activate the NRF2/FPN1 signaling pathway. As expected, we found that activation of NRF2 can distinctly alleviate myocardial IRI in diabetic rats. SFN significantly improved post-myocardial IRI cardiac functional recovery by increasing LVEF and LVFS, the size of myocardial infarction was also reduced ($P< 0.05$). While the ferroptosis agonist Erastin attenuated cardioprotective effect of SFN (Fig. 3A-B). The LDH and CK-MB levels in the DIR+SFN group were lower compared with the DIR group (Fig. 3C), indicate that the degree of myocardial IRI was reduced. Through HE staining observation, compared with the DIR group, the left ventricular ultrastructure and the level of interstitial myocardial fibrosis in the DIR+SFN group were reduced (Fig. 3D).

Western blot and qRT-PCR showed that after pretreatment with SFN, the expression of NRF2, FPN1 and GPX4 in rat myocardium were up-regulated, the expression of ACSL4 was down-regulated (Fig. 3E-F). When exposed to Erastin treatment, the above effects of SFN were all inhibited, and the expression of GPX4 was lower than that in DIR+SFN group, but the expression of ACSL4 was higher (Fig. 3A-F). These results collectively suggest that the protective effect on myocardial IRI by activating the NRF2/FPN1 signaling pathway is achieved through inhibition of ferroptosis.

### Downregulation of NRF2/FPN1 pathway is accompanied by ferroptosis in H9c2 cardiomyocytes exposed to HH/R

To identify further molecular mechanism of NRF2/FPN1 pathway in diabetic myocardial IRI, H9c2 cardiomyocytes were used for in vivo experiments. Compared with normal group, the cell viability of H9c2 cells in HG group and H/R group were decreased, and lipid ROS production were increased (Fig. 4A-B). HG and H/R treatment could increase intracellular $Fe^{2+}$ and MDA content and decrease SOD activity (Fig. 4C). And the above changes were more obvious in the HH/R group ($P< 0.05$). The conditions were consistent with in vitro experiments, HG and H/R treatment down-regulated the expression of NRF2, FPN1 and GPX4 at the same time up-regulated the expression of ACSL4 (Fig. 4D-E). From these findings we can infer that hypo-expression of the NRF2/FPN1 signaling pathway in H9c2 cardiomyocytes exposed to HH/R could cause iron over-load and lipid peroxide accumulation, which in turn results in ferroptosis.

### The protective effects of NRF2 agonist SFN in H9c2 cardiomyocytes from HH/R-induced ferroptosis were reversed by Erastin

To identify the possible mechanisms underlying the protective effects of NRF2 in HH/R-induced ferroptosis, H9c2 cardiomyocytes overexpressing NRF2 were obtained via administration with SFN. As depicted in Fig. S1 A-B, compared to the other groups, the HH/R and SFN treatment group showed more

significant upregulation of NRF2/FPN1 signaling pathway and more pronounced changes in ferroptosis-related proteins ($P< 0.05$). Therefore, in line with our expectations, we focused our study mainly on the HH/R group. As showed in Fig. 5A, the cell viability was increased in the HH/R+SFN group. Compared with HH/R group, the ROS fluorescence intensity were significantly reduced after SFN incubation (Fig. 5B). Besides, SFN treatment significantly attenuated intracellular $Fe^{2+}$ content and lipid peroxide accumulation by impacting SOD and MDA levels (Fig. 5C). After NRF2 was activated by SFN, the expression of iron metabolism-related protein FPN1 were also increased accordingly, with reduced indicators of ferroptosis (Fig. 5D-E). Furthermore, as seen in Fig. 5A-E, after pretreatment with Erastin, the expression of NRF2 and FPN1 did not change significantly with increased ferroptosis level ($P> 0.05$). Collectively, ferroptosis agonist reversed the beneficial effect of overexpression of NRF2/FPN1 signaling pathway to protect H9c2 cardiomyocytes from HH/R-induced ferroptosis.

### NRF2 agonist SFN protects H9c2 cardiomyocytes from HH/R-induced ferroptosis by transcribing downstream iron metabolism-related gene via nuclear translocation

NRF2, a key regulator of the cellular antioxidant defense system, plays a beneficial role in balancing the oxidative stress status in cells. And in the nucleus, NRF2 acts as a transcription factor to regulate iron metabolism-related gene SLC40A1. Therefore, to visualize the nuclear localization of NRF2, an immunofluorescence assay was performed in H9c2 cardiomyocytes. As presented in Fig. 6, compared with normal group, there was a significant decrease in NRF2 protein expression in the nucleus relative to the cytoplasm following the treatment of HH/R ($P< 0.05$). Moreover, SFN pretreatment significantly increased the nuclear translocation of NRF2 ($P< 0.05$). Taken together, these data suggested that SFN protect H9c2 cardiomyocytes from ferroptosis damage by modulating NRF2 nuclear accumulation..

## Discussion

In this study, we attempted at understanding whether ferroptosis, an iron-dependent regulated form of cell death caused by iron dysmetabolism and accumulation of lipid peroxides, may underlie the pathogenesis of myocardial IRI in diabetic rats. Furthermore, we first evaluated whether the activation of NRF2/FPN1 signal pathway could prevent ferroptosis in diabetic myocardial IRI. In addition, nuclear transfer of NRF2 plays a pivotal role in ferroptosis in STZ-induced diabetic IRI. To our knowledge, this is the first study to examine the mechanism of NRF2-mediated cardio-protection by regulating iron metabolic balance and iron homeostasis.

In the present study, we respectively established rat diabetes and ischemia-reperfusion models to simulate myocardial ischemia-reperfusion in diabetic patients. For the in vivo experiments, it was obviously showed that diabetes can increase the vulnerability of the heart following ischemia-reperfusion. When the body's tissues or organs are damaged, cellular metabolism gets affected and PH decreases, resulting in the reduction of intracellular $Fe^{3+}$ to $Fe^{2+}$, overloaded iron ions can form highly reactive and toxic hydroxyl radicals via the Haber-Weiss/Fenton reactions, which in turn can cause ferroptosis[24]. Furthermore, related research have shown that supply of exogenous iron such as ferric

ammonium citrate, ammonium citrate and ferric citrate can enhance the ferroptosis induced by erastin and RSL3[25], while the antioxidant vitamin E can inhibit ferroptosis[26]. It is thus clear that iron metabolic homeostasis and oxidative stress play important roles in the pathogenesis of ferroptosis. Malondialdehyde is the end product of membrane lipid peroxidation reaction, which can reflect the degree of initiation of lipid peroxidation reaction. Superoxide dismutase, which is commonly found in aerobic organisms, is an important member of the antioxidant enzyme class and is one of the main enzymes for effective scavenging of ROS in organisms. By measuring the content of $Fe^{2+}$, SOD and MDA in myocardial tissues, our study found iron ions accumulation and imbalance of oxidative and antioxidant systems in rat hearts under diabetes and myocardial IR conditions. We therefore speculate that ferroptosis may have occurred during diabetic myocardial IRI. Acyl-CoA synthetase long-chain family member 4 (ACSL4) is a reliable marker of ferroptosis and induces the production of the signature signal of ferroptosis, 5-hydroxyeicosatetraenoic acid (5-HETE)[27]. GPX4 is the only enzyme in the GPX family that reduces esterification of oxidized fatty acids and cholesterol hydroperoxides[28]. As we expected, the mRNA and protein expression of ACSL4 and GPX4 are changed during diabetic myocardial IRI, which is in line with previous reports[29, 30]. From these, we confirm that the increased vulnerability of myocardial IRI in diabetic patients is strongly linked to the disorders of iron metabolism and ferroptosis, which was consistent with studies that found ferroptosis in diabetic myocardial IRI[31, 32].

A growing number of experimental studies have illustrated that NRF2 can attenuate diabetic myocardial IRI and effectuate cardioprotective effects[33]. In present study, our results showed that the level of NRF2 was downregulated after IR induction as well as during hyperglycemic states, which was consistent with the conclusion of Liu et al[34]. and Tan et al[35]. Therefore, we inferred that the down-regulation of NRF2 expression in the diabetic heart exacerbates oxidative stress and insulin resistance, resulting in exacerbation of myocardial damage. SFN is a well-studied classic NRF2 agonist that prevents oxidative stress injury and the accompanying cardiovascular disease. In consideration of the fact that the pathogenesis of diabetic cardiomyopathy is a complex chronic process, fast drug administration of SFN has limited cardioprotection in diabetic rats. Consequently, we refer to Piao et al. who chose to inject SFN (500μg/kg/day) intraperitoneally for 3 consecutive days before ischemia[19]. Our study showed that SFN administration significantly attenuated diabetic myocardial IRI, as evidenced by reduced infarct size, lower serum biomarker levels, and preservation of cardiac function. Additionally, our data suggested that compared with the DIR group, NRF2, FPN1 and GPX4 expression was upregulated, ACSL4 expression was downregulated, myocardial $Fe^{2+}$ and MDA content was decreased, and SOD activity was increased in the DIR+SFN group, indicating that SFN can reduce myocardial IRI in diabetic rats by promoting FPN1-mediated $Fe^{2+}$ efflux and in turn limiting ferroptosis.

To further test our hypothesis, the specific mechanism was verified in H9c2 cells in detail. There has been a lot of studies showed the involvement of oxidative stress in diabetes as well as in myocardial IRI[30]. And it was confirmed that ROS could directly or indirectly cause cells necrosis and tissues damage[36]. Consistent with in vivo experimental results, H9c2 cells stimulated by HG or H/R were subjected to severe damage, simultaneously its ROS levels was increased. However, the mRNA and protein expression of

NRF2 and FPN1 were decreased. This is consistent with the findings of Xu et al[37]. We consider that it may be due to the fact that diabetic heart disease is a chronic disease model where long-term oxidative stress depletes antioxidant elements such as NRF2. In further study, the application of SFN rescues this situation and thus alleviates HH/R injury in H9c2 cells. Notably, it has been recently shown that altered expression of NRF2 in the nucleus can affect its transcriptional target FPN1, which in turn ultimately leads to the reduction of iron efflux and the increased intracellular iron content[38]. Similarly, in our study, our cellular immunofluorescent analysis suggests that NRF2 translocates from the cytoplasm to the nucleus in the process of H9c2 cells damage induced by HG or H/R, thereby activating the transcription of its target gene FPN1 to limit ferroptosis. Overall, in response to oxidative stress, we speculated that NRF2 is released from the cytoplasm and translocated into the nucleus, where it binds to the upstream promoter region of the antioxidant response element (ARE) and members of the sMaf protein family. As shown in Fig. 7, the above process eventually resulted in transcription of downstream protective protein genes like FPN1 and heightened cellular resistance to ferroptosis.

Erastin, a ferroptosis inducer acting on the Xc-system, is currently accepted as the most commonly used ferroptosis inducer[39]. Intriguingly, our experiment results indicated that the use of erastin blocked the beneficial effects of SFN and increased the degree of ferroptosis, but did not affect the expression of NRF2 and FPN1, which also verified that ferroptosis is controlled by targeting the NRF2/FPN1 signaling pathway. Together, we can conclude that hypo-expression of FPN1 can lead to intracellular iron accumulation and aggravate ferroptosis in the diabetic heart disease, and that SFN further stimulates NRF2 to promote the transcription of FPN1 and reduce myocardial IRI in diabetic rats.

There are some limitations to this study. On the one hand, our study is limited to STZ-induced type 1 diabetic rats. As type 2 diabetes is the most common form of diabetes, it is of great value to assess the critical role of the NRF2/FPN1 signaling pathway in this condition. On the other hand, because of the technical limitations of the experiment, we were not able to successfully extract the NRF2 in the nucleus of the cells. Although the transcriptional action of NRF2 is achieved in the nucleus, no studies until now have clearly shown the extent of translocation of NRF2 from the cytoplasm to the nucleus, that is also the main reason why we finally chose to extract the total NRF2. Precisely for these reasons, further study is still needed to reveal the underlying molecular mechanism.

In conclusion, our present study demonstrated that NRF2/FPN1 signal pathway is a pivotal mechanism in diabetic myocardial IRI by regulating iron metabolic homeostasis to restrict ferroptosis, and activation of NRF2/FPN1 signal pathway can relieve diabetic myocardial IRI to some extent. Modulating ferroptosis by impacting iron metabolism may provide an effective strategy for the prophylaxis and treatment of diabetic myocardial IRI.

# Declarations


### Acknowledgement

This study was supported by grants from the National Natural Science Foundation of China (81970722). The authors would like to thank the Central Laboratory, Renmin Hospital of Wuhan University (Wuhan, Hubei, China) for their support of our study.

### Declaration of competing interest

The authors assert that they have no known competing financial interests or personal relationships.

### Author contributions

H. Tian designed this study, performed major parts of the experiments and wrote the manuscript; Y. Zhang and Y. H. Xiong helped in experimental design; J. Tao and L. Li participated in in vivo experiments and western blot experiments; Y. Leng participated in the interpretation of our results; Z. Y. Xia and Z. Qiu developed the concept and provided guidance during the study.

### Ethical Approval

All applicable international, national, and/or institutional guidelines for the care and use of animals were followed.

### Data availability statements

All data generated or analysed during this study are included in this published article (and its supplementary information files).

## References

1. Davidson SM, Ferdinandy P, Andreadou I, Bøtker HE, Heusch G, Ibáñez B, Ovize M, Schulz R, Yellon DM, Hausenloy DJ *et al*: Multitarget Strategies to Reduce Myocardial Ischemia/Reperfusion Injury: JACC Review Topic of the Week. *Journal of the American College of Cardiology* 2019, 73(1):89–99.doi:10.1016/j.jacc.2018.09.086
2. Zhang Y, Liu D, Hu H, Zhang P, Xie R, Cui W: HIF-1α/BNIP3 signaling pathway-induced-autophagy plays protective role during myocardial ischemia-reperfusion injury. *Biomedicine & pharmacotherapy = Biomedecine & pharmacotherapie* 2019, 120:109464.doi:10.1016/j.biopha.2019.109464
3. Fan Q, Tao R, Zhang H, Xie H, Lu L, Wang T, Su M, Hu J, Zhang Q, Chen Q *et al*: Dectin-1 Contributes to Myocardial Ischemia/Reperfusion Injury by Regulating Macrophage Polarization and Neutrophil Infiltration. *Circulation* 2019, 139(5):663–678.doi:10.1161/circulationaha.118.036044
4. Zhai M, Li B, Duan W, Jing L, Zhang B, Zhang M, Yu L, Liu Z, Yu B, Ren K *et al*: Melatonin ameliorates myocardial ischemia reperfusion injury through SIRT3-dependent regulation of oxidative stress and apoptosis. *Journal of pineal research* 2017, 63(2).doi:10.1111/jpi.12419
5. Dixon SJ, Lemberg KM, Lamprecht MR, Skouta R, Zaitsev EM, Gleason CE, Patel DN, Bauer AJ, Cantley AM, Yang WS *et al*: Ferroptosis: an iron-dependent form of nonapoptotic cell death. *Cell*

2012, 149(5):1060–1072.doi:10.1016/j.cell.2012.03.042

6. Galluzzi L, Vitale I, Abrams JM, Alnemri ES, Baehrecke EH, Blagosklonny MV, Dawson TM, Dawson VL, El-Deiry WS, Fulda S *et al*: Molecular definitions of cell death subroutines: recommendations of the Nomenclature Committee on Cell Death 2012. *Cell death and differentiation* 2012, 19(1):107–120.doi:10.1038/cdd.2011.96
7. Gozzelino R, Arosio P: Iron Homeostasis in Health and Disease. *International journal of molecular sciences* 2016, 17(1).doi:10.3390/ijms17010130
8. Lakhal-Littleton S, Wolna M, Carr CA, Miller JJ, Christian HC, Ball V, Santos A, Diaz R, Biggs D, Stillion R *et al*: Cardiac ferroportin regulates cellular iron homeostasis and is important for cardiac function. *Proceedings of the National Academy of Sciences of the United States of America* 2015, 112(10):3164–3169.doi:10.1073/pnas.1422373112
9. Kasztura M, Dzięgała M, Kobak K, Bania J, Mazur G, Banasiak W, Ponikowski P, Jankowska EA: Both iron excess and iron depletion impair viability of rat H9C2 cardiomyocytes and L6G8C5 myocytes. *Kardiologia polska* 2017, 75(3):267–275.doi:10.5603/KP.a2016.0155
10. Harada N, Kanayama M, Maruyama A, Yoshida A, Tazumi K, Hosoya T, Mimura J, Toki T, Maher JM, Yamamoto M *et al*: Nrf2 regulates ferroportin 1-mediated iron efflux and counteracts lipopolysaccharide-induced ferroportin 1 mRNA suppression in macrophages. *Archives of biochemistry and biophysics* 2011, 508(1):101–109.doi:10.1016/j.abb.2011.02.001
11. Moi P, Chan K, Asunis I, Cao A, Kan YW: Isolation of NF-E2-related factor 2 (Nrf2), a NF-E2-like basic leucine zipper transcriptional activator that binds to the tandem NF-E2/AP1 repeat of the beta-globin locus control region. *Proceedings of the National Academy of Sciences of the United States of America* 1994, 91(21):9926–9930.doi:10.1073/pnas.91.21.9926
12. Brownlee M: The pathobiology of diabetic complications: a unifying mechanism. *Diabetes* 2005, 54(6):1615–1625.doi:10.2337/diabetes.54.6.1615
13. Ichihara S: The pathological roles of environmental and redox stresses in cardiovascular diseases. *Environmental health and preventive medicine* 2013, 18(3):177–184.doi:10.1007/s12199-012-0326-2
14. Zhang B, Zhai M, Li B, Liu Z, Li K, Jiang L, Zhang M, Yi W, Yang J, Yi D *et al*: Honokiol Ameliorates Myocardial Ischemia/Reperfusion Injury in Type 1 Diabetic Rats by Reducing Oxidative Stress and Apoptosis through Activating the SIRT1-Nrf2 Signaling Pathway. *Oxidative medicine and cellular longevity* 2018, 2018:3159801.doi:10.1155/2018/3159801
15. Liu Z, Han K, Huo X, Yan B, Gao M, Lv X, Yu P, Gao G, Chang YZ: Nrf2 knockout dysregulates iron metabolism and increases the hemolysis through ROS in aging mice. *Life sciences* 2020, 255:117838.doi:10.1016/j.lfs.2020.117838
16. La Rosa P, Petrillo S, Turchi R, Berardinelli F, Schirinzi T, Vasco G, Lettieri-Barbato D, Fiorenza MT, Bertini ES, Aquilano K *et al*: The Nrf2 induction prevents ferroptosis in Friedreich's Ataxia. *Redox biology* 2021, 38:101791.doi:10.1016/j.redox.2020.101791

17. Luo LF, Guan P, Qin LY, Wang JX, Wang N, Ji ES: Astragaloside IV inhibits adriamycin-induced cardiac ferroptosis by enhancing Nrf2 signaling. *Molecular and cellular biochemistry* 2021.doi:10.1007/s11010-021-04112-6
18. Qiu Z, Lei S, Zhao B, Wu Y, Su W, Liu M, Meng Q, Zhou B, Leng Y, Xia ZY: NLRP3 Inflammasome Activation-Mediated Pyroptosis Aggravates Myocardial Ischemia/Reperfusion Injury in Diabetic Rats. *Oxidative medicine and cellular longevity* 2017, 2017:9743280.doi:10.1155/2017/9743280
19. Piao CS, Gao S, Lee GH, Kim DS, Park BH, Chae SW, Chae HJ, Kim SH: Sulforaphane protects ischemic injury of hearts through antioxidant pathway and mitochondrial K(ATP) channels. *Pharmacological research* 2010, 61(4):342–348.doi:10.1016/j.phrs.2009.11.009
20. Xiao C, Xia ML, Wang J, Zhou XR, Lou YY, Tang LH, Zhang FJ, Yang JT, Qian LB: Luteolin Attenuates Cardiac Ischemia/Reperfusion Injury in Diabetic Rats by Modulating Nrf2 Antioxidative Function. *Oxidative medicine and cellular longevity* 2019, 2019:2719252.doi:10.1155/2019/2719252
21. Fang X, Wang H, Han D, Xie E, Yang X, Wei J, Gu S, Gao F, Zhu N, Yin X *et al*: Ferroptosis as a target for protection against cardiomyopathy. *Proceedings of the National Academy of Sciences of the United States of America* 2019, 116(7):2672–2680.doi:10.1073/pnas.1821022116
22. Marro S, Chiabrando D, Messana E, Stolte J, Turco E, Tolosano E, Muckenthaler MU: Heme controls ferroportin1 (FPN1) transcription involving Bach1, Nrf2 and a MARE/ARE sequence motif at position -7007 of the FPN1 promoter. *Haematologica* 2010, 95(8):1261–1268.doi:10.3324/haematol.2009.020123
23. Donovan A, Lima CA, Pinkus JL, Pinkus GS, Zon LI, Robine S, Andrews NC: The iron exporter ferroportin/Slc40a1 is essential for iron homeostasis. *Cell metabolism* 2005, 1(3):191–200.doi:10.1016/j.cmet.2005.01.003
24. Qi X, Zhang Y, Guo H, Hai Y, Luo Y, Yue T: Mechanism and intervention measures of iron side effects on the intestine. *Critical reviews in food science and nutrition* 2020, 60(12):2113–2125.doi:10.1080/10408398.2019.1630599
25. Manz DH, Blanchette NL, Paul BT, Torti FM, Torti SV: Iron and cancer: recent insights. *Annals of the New York Academy of Sciences* 2016, 1368(1):149–161.doi:10.1111/nyas.13008
26. Kagan VE, Mao G, Qu F, Angeli JP, Doll S, Croix CS, Dar HH, Liu B, Tyurin VA, Ritov VB *et al*: Oxidized arachidonic and adrenic PEs navigate cells to ferroptosis. *Nature chemical biology* 2017, 13(1):81–90.doi:10.1038/nchembio.2238
27. Yuan H, Li X, Zhang X, Kang R, Tang D: Identification of ACSL4 as a biomarker and contributor of ferroptosis. *Biochemical and biophysical research communications* 2016, 478(3):1338–1343.doi:10.1016/j.bbrc.2016.08.124
28. Doll S, Freitas FP, Shah R, Aldrovandi M, da Silva MC, Ingold I, Goya Grocin A, Xavier da Silva TN, Panzilius E, Scheel CH *et al*: FSP1 is a glutathione-independent ferroptosis suppressor. *Nature* 2019, 575(7784):693–698.doi:10.1038/s41586-019-1707-0
29. Wang C, Zhu L, Yuan W, Sun L, Xia Z, Zhang Z, Yao W: Diabetes aggravates myocardial ischaemia reperfusion injury via activating Nox2-related programmed cell death in an AMPK-dependent manner.

*Journal of cellular and molecular medicine* 2020, 24(12):6670–6679.doi:10.1111/jcmm.15318

30. Zhao D, Yang J, Yang L: Insights for Oxidative Stress and mTOR Signaling in Myocardial Ischemia/Reperfusion Injury under Diabetes. *Oxidative medicine and cellular longevity* 2017, 2017:6437467.doi:10.1155/2017/6437467
31. Li W, Li W, Leng Y, Xiong Y, Xia Z: Ferroptosis Is Involved in Diabetes Myocardial Ischemia/Reperfusion Injury Through Endoplasmic Reticulum Stress. *DNA and cell biology* 2020, 39(2):210–225.doi:10.1089/dna.2019.5097
32. Tang LJ, Luo XJ, Tu H, Chen H, Xiong XM, Li NS, Peng J: Ferroptosis occurs in phase of reperfusion but not ischemia in rat heart following ischemia or ischemia/reperfusion. *Naunyn-Schmiedeberg's archives of pharmacology* 2021, 394(2):401–410.doi:10.1007/s00210-020-01932-z
33. Zhou XR, Ru XC, Xiao C, Pan J, Lou YY, Tang LH, Yang JT, Qian LB: Sestrin2 is involved in the Nrf2-regulated antioxidative signaling pathway in luteolin-induced prevention of the diabetic rat heart from ischemia/reperfusion injury. *Food & function* 2021, 12(8):3562–3571.doi:10.1039/d0fo02942d
34. Liu Z, Zhang F, Zhao L, Zhang X, Li Y, Liu L: Protective Effect of Pravastatin on Myocardial Ischemia Reperfusion Injury by Regulation of the miR-93/Nrf2/ARE Signal Pathway. *Drug design, development and therapy* 2020, 14:3853–3864.doi:10.2147/dddt.S251726
35. Tan Y, Ichikawa T, Li J, Si Q, Yang H, Chen X, Goldblatt CS, Meyer CJ, Li X, Cai L *et al*: Diabetic downregulation of Nrf2 activity via ERK contributes to oxidative stress-induced insulin resistance in cardiac cells in vitro and in vivo. *Diabetes* 2011, 60(2):625–633.doi:10.2337/db10-1164
36. Ma Q: Transcriptional responses to oxidative stress: pathological and toxicological implications. *Pharmacology & therapeutics* 2010, 125(3):376–393.doi:10.1016/j.pharmthera.2009.11.004
37. Xu G, Zhao X, Fu J, Wang X: Resveratrol increase myocardial Nrf2 expression in type 2 diabetic rats and alleviate myocardial ischemia/reperfusion injury (MIRI). *Annals of palliative medicine* 2019, 8(5):565–575.doi:10.21037/apm.2019.11.25
38. Yang S, Deng Q, Sun L, Dong K, Li Y, Wu S, Huang R: Salmonella effector SpvB interferes with intracellular iron homeostasis via regulation of transcription factor NRF2. *FASEB journal: official publication of the Federation of American Societies for Experimental Biology* 2019, 33(12):13450–13464.doi:10.1096/fj.201900883RR
39. Yang Y, Luo M, Zhang K, Zhang J, Gao T, Connell DO, Yao F, Mu C, Cai B, Shang Y *et al*: Nedd4 ubiquitylates VDAC2/3 to suppress erastin-induced ferroptosis in melanoma. *Nature communications* 2020, 11(1):433.doi:10.1038/s41467-020-14324-x

# Figures

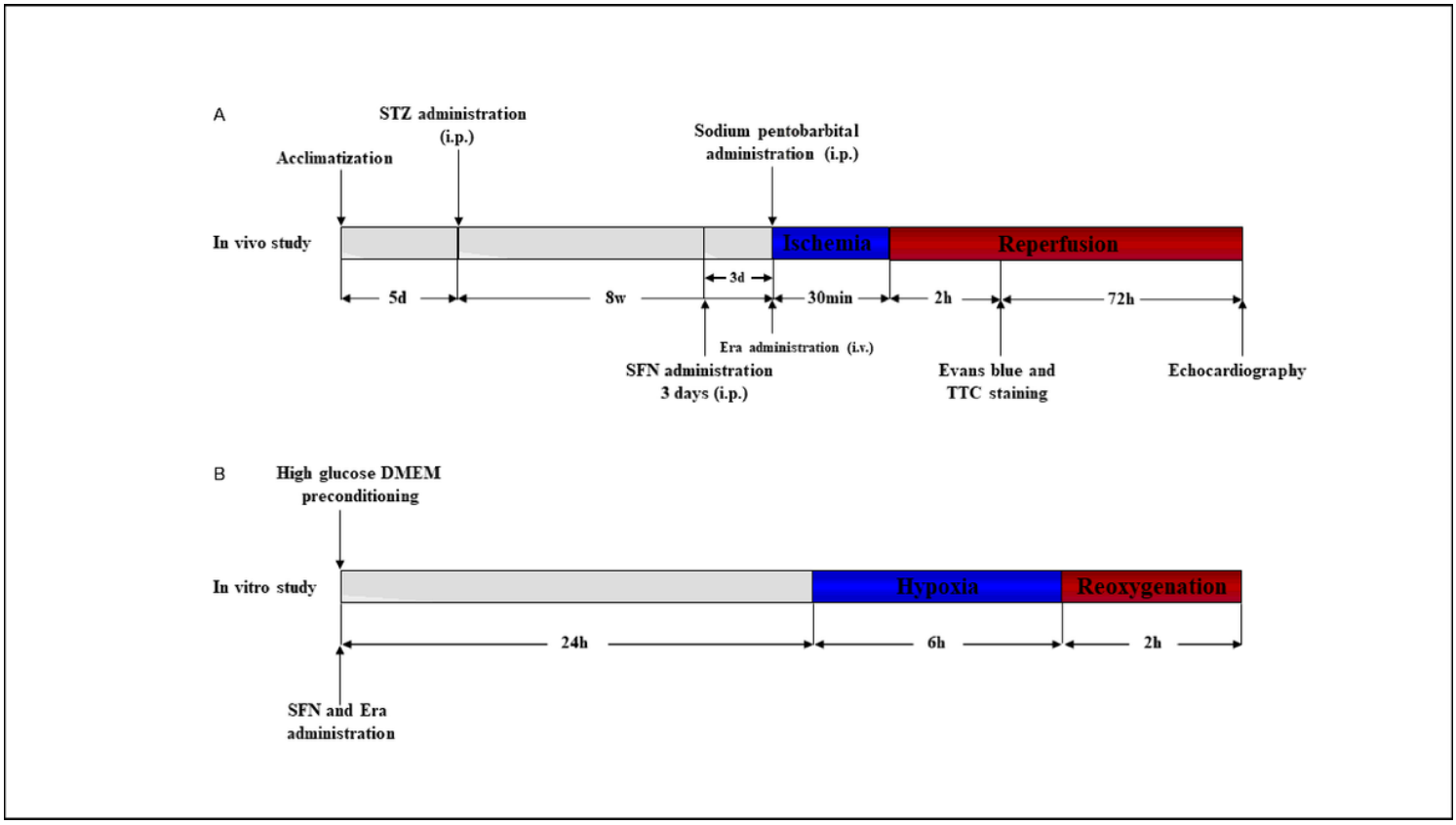


## Figure 1

Experimental protocols. Illustration showing the experimental procedures including diabetes induction, ischemia-reperfusion model, SFN and Era administration, and sacrifice end point. (A) In vivo experimental protocol. (B) In vitro experimental protocol. STZ: streptozotocin. SFN:sulforaphane. Era:erastin.

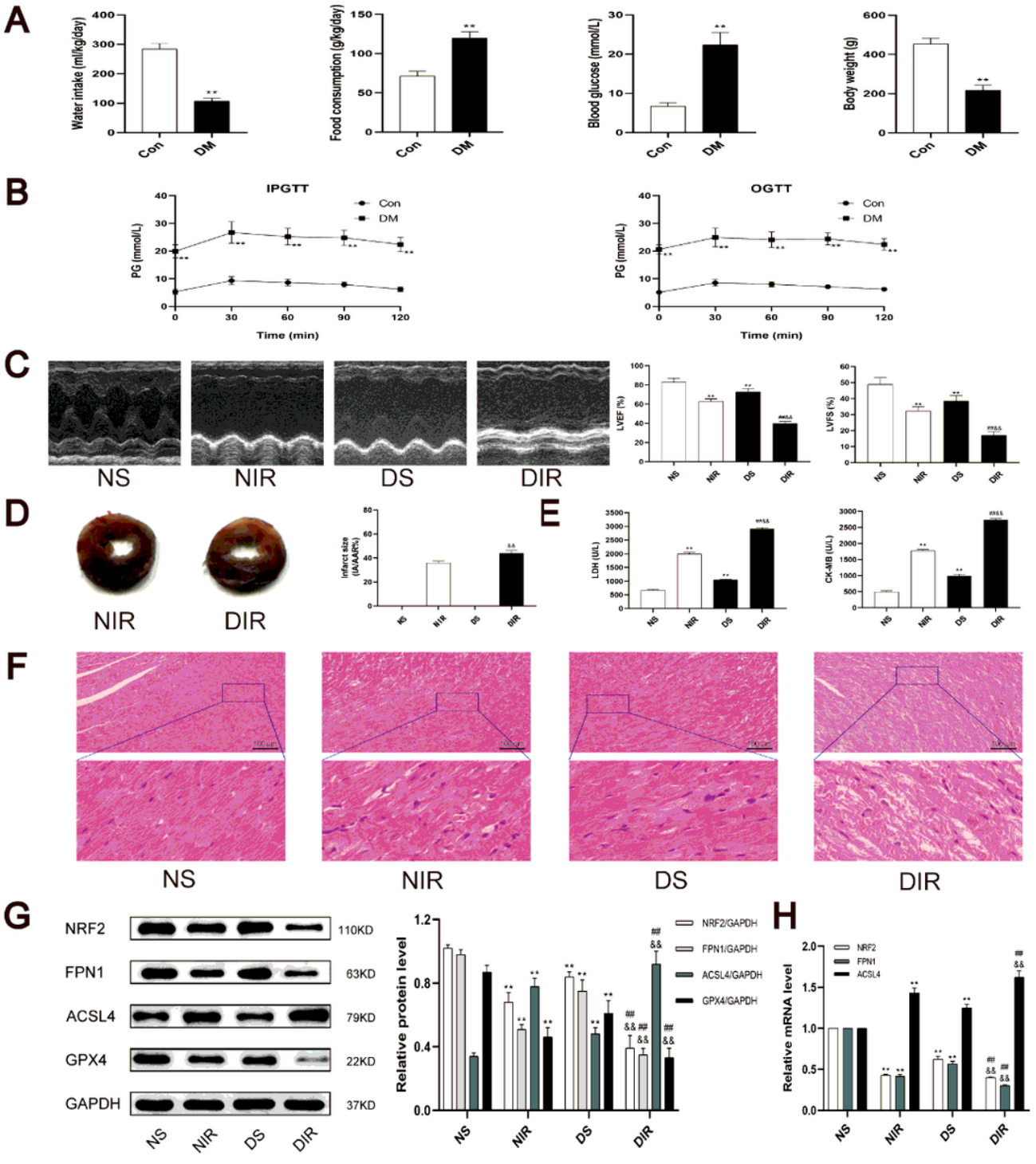


## Figure 2

The effects of diabetes and myocardial IRI on ferroptosis and NRF2 pathway. (A) Basic characteristics of diabetic rats. Water intake and food consumption were the average value of 8 weeks. Body weight and plasma glucose were recorded before inducing myocardial ischemia-reperfusion. (B) Intraperitoneal glucose tolerance test and oral glucose tolerance test of diabetic rats. (C) Representative M-mode images by echocardiography. (D) Infarct size was detected by TTC. (E) The levels of CK-MB and LDH in serum were detected. (F) Histopathological changes of myocardium were detected by HE staining. (G) The

protein levels of NRF2, FPN1, ACSL4 and GPX4 in myocardial tissue were detected by western blot. (H) The mRNA levels of NRF2, ACSL4 and GPX4 in myocardial tissue were detected by qRT-PCR. The results are expressed as the means ± SD. N=8 for each group. **P< 0.05 vs. NS group. ##P< 0.05 vs. NIR group. &&P< 0.05 vs. DS group.

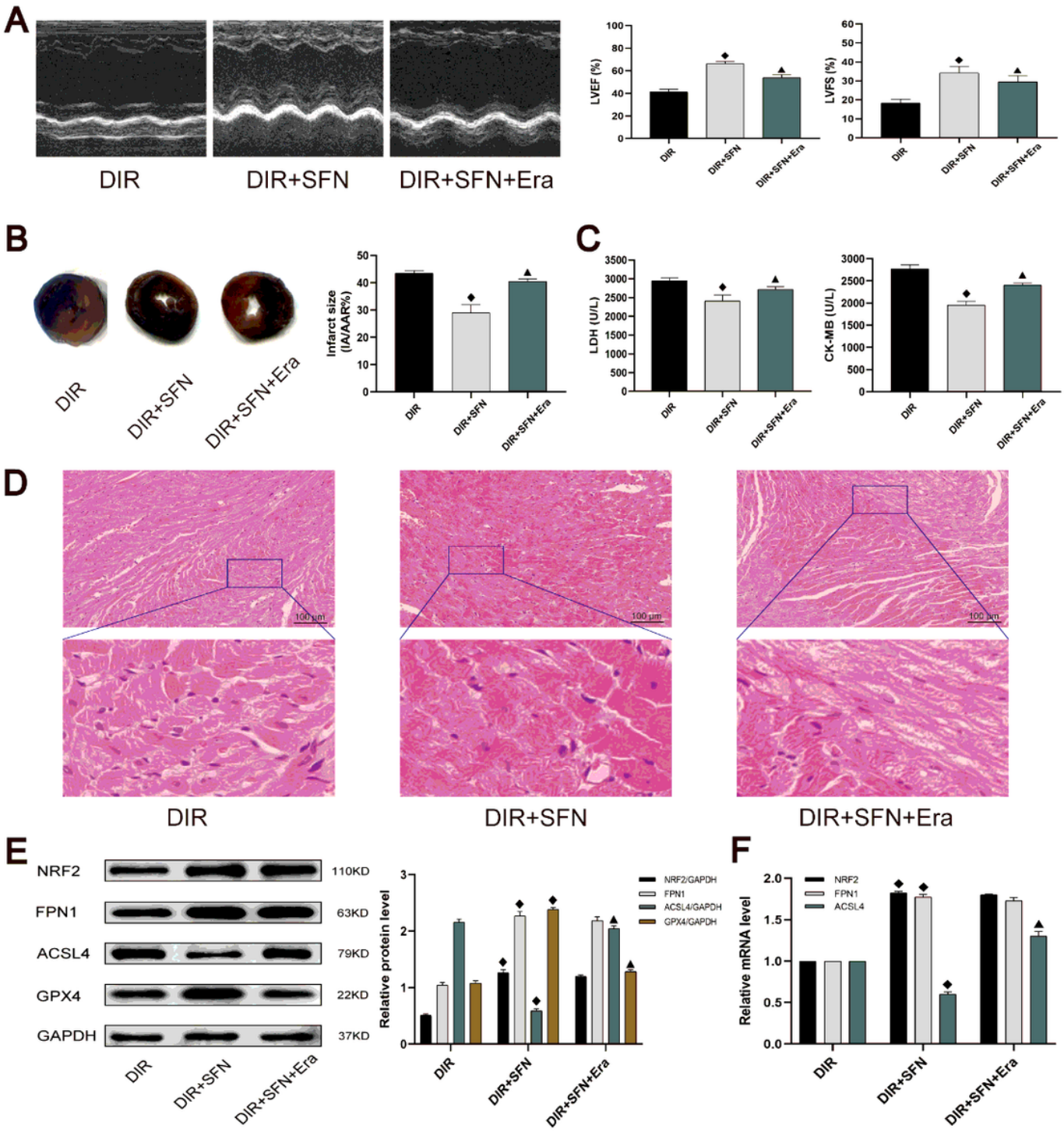


## Figure 3

The ferroptosis agonist could abrogate the protective effect of NRF2 agonist SFN in diabetic rats following myocardial IRI. (A) Representative M-mode images by echocardiography. (B) Infarct size was

detected by TTC. (C) The levels of CK-MB and LDH in serum were detected. (D) Histopathological changes of myocardium were detected by HE staining. (E) The protein levels of NRF2, FPN1, ACSL4 and GPX4 in myocardial tissue were detected by western blot. (F) The mRNA levels of NRF2, ACSL4 and GPX4 in myocardial tissue were detected by qRT-PCR. The results are expressed as the means ± SD. N=8 for each group. ▯P< 0.05 vs. DIR group. ▲P< 0.05 vs. DIR+SFN group.

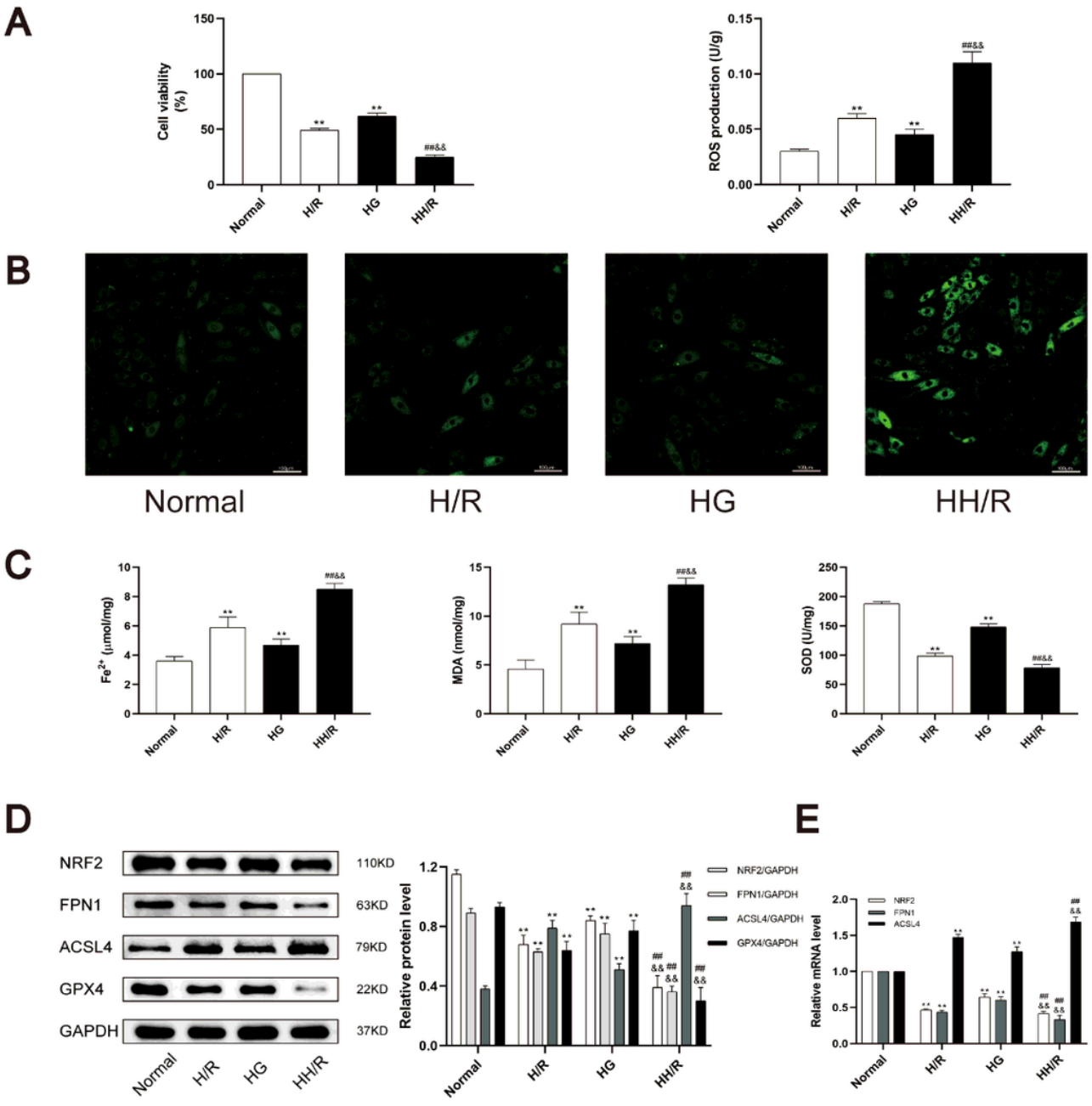


Figure 4

Downregulation of NRF2/FPN1 pathway is accompanied by ferroptosis in H9c2 cardiomyocytes exposed to HH/R. (A) Cell viability was detected by CCK-8. (B) ROS production was measured by adding the fluorescent probes to the cells during 20 min at 37°C. Scale bars: 100μm. (C) Fe2+content, MDA and SOD levels in H9c2 cells were detected. (D) The protein levels of NRF2, FPN1, ACSL4 and GPX4 in myocardial tissue were detected by western blot. (E) The mRNA levels of NRF2, ACSL4 and GPX4 in myocardial tissue were detected by qRT-PCR. **P< 0.05 vs. NS group. ##P< 0.05 vs. NIR group. &&P< 0.05 vs. DS group.

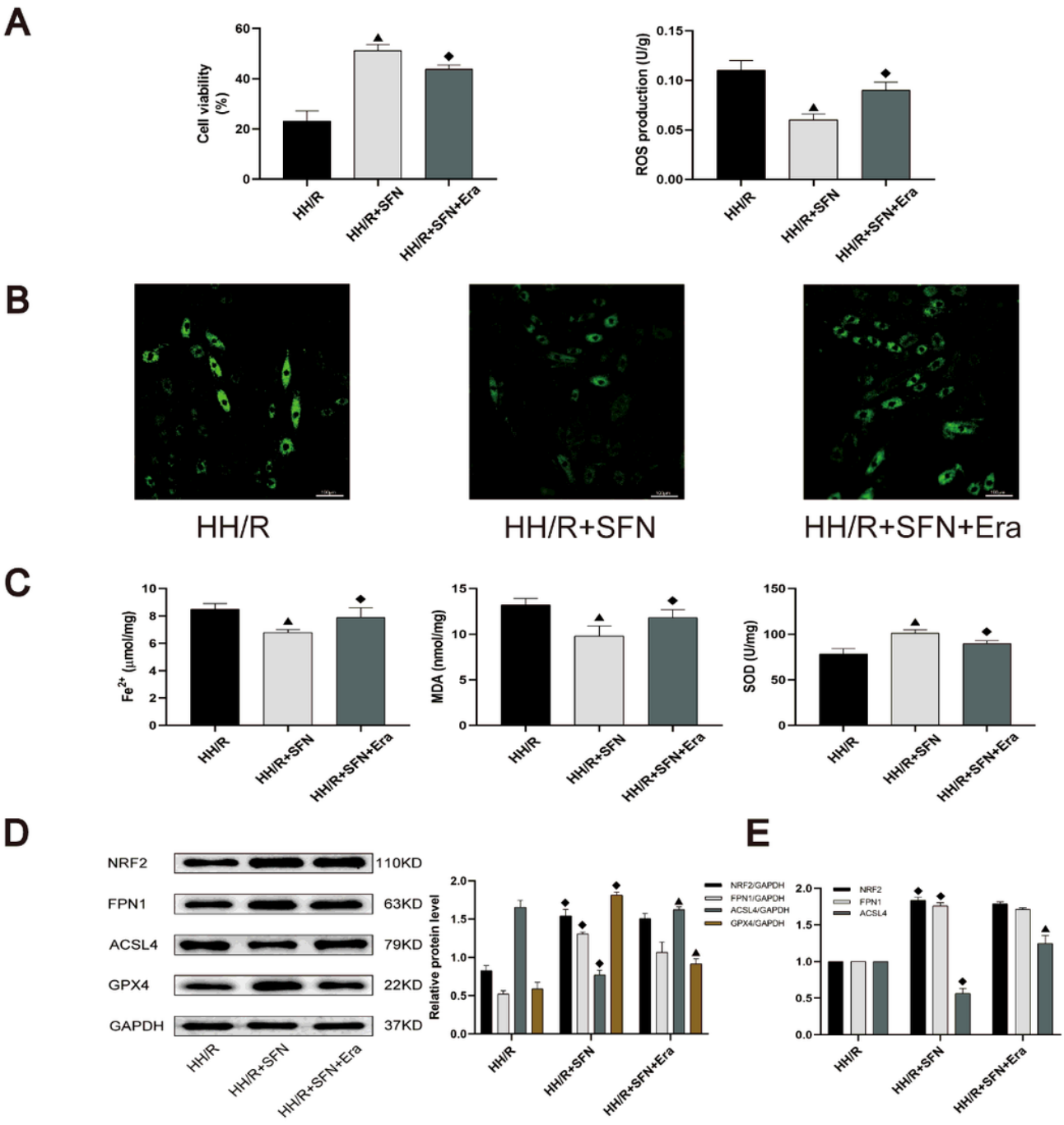


**Figure 5**

The protective effects of NRF2 agonist SFN in H9c2 cardiomyocytes from HH/R-induced ferroptosis were reversed by Erastin. (A) Cell viability was detected by CCK-8. (B) ROS production was measured by adding the fluorescent probes to the cells during 20 min at 37℃. Scale bars: 100μm. (C) Fe2+content, MDA and SOD levels in H9c2 cells were detected. (D) The protein levels of NRF2, FPN1, ACSL4 and GPX4 in myocardial tissue were detected by western blot. (E) The mRNA levels of NRF2, ACSL4 and GPX4 in myocardial tissue were detected by qRT-PCR. ▯P< 0.05 vs. DIR group. ▲P< 0.05 vs. DIR+SFN group.

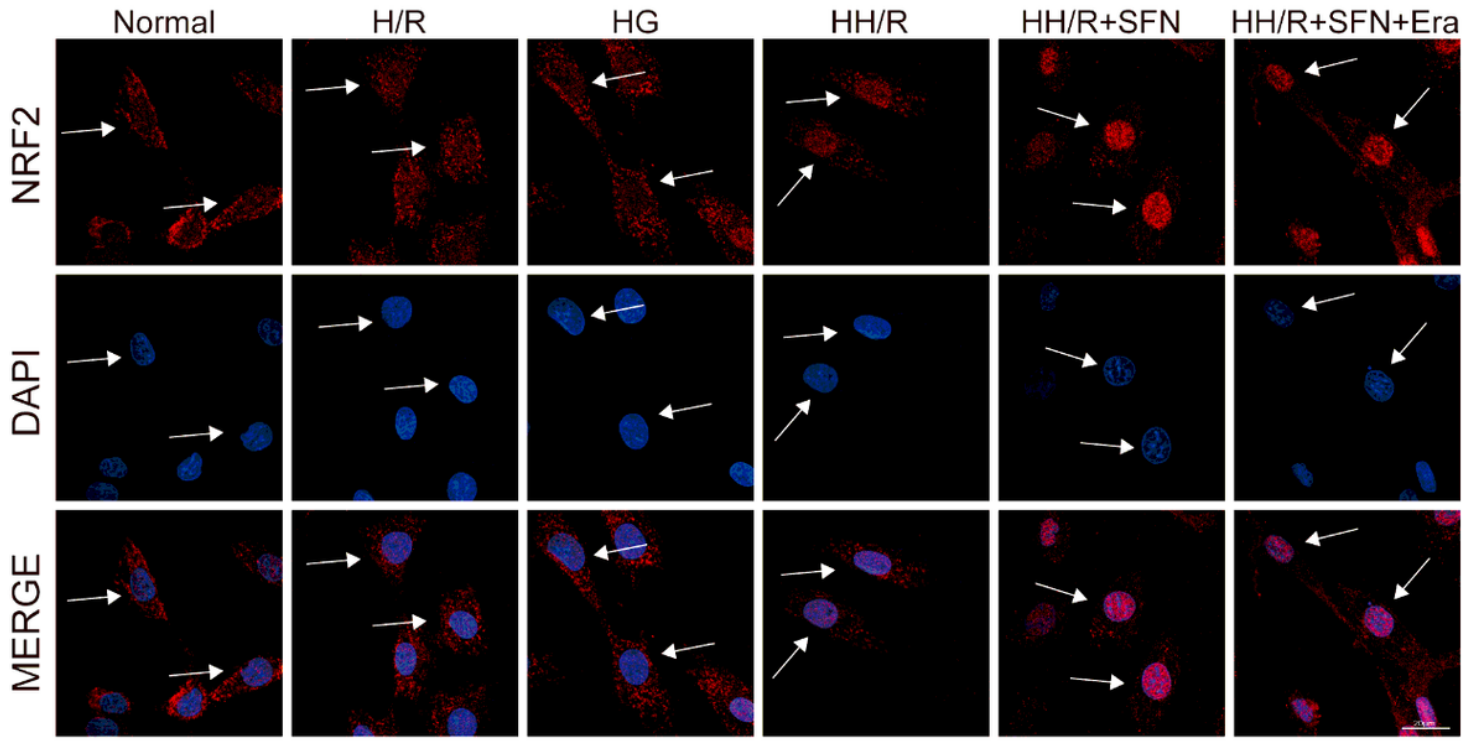


## Figure 6

Immunofluorescence staining of NRF2 using H9c2 cardiomyocytes after corresponding stimulation. The red dots represents NRF2, and blue dots shows nuclear. Scale bars: 20μm.

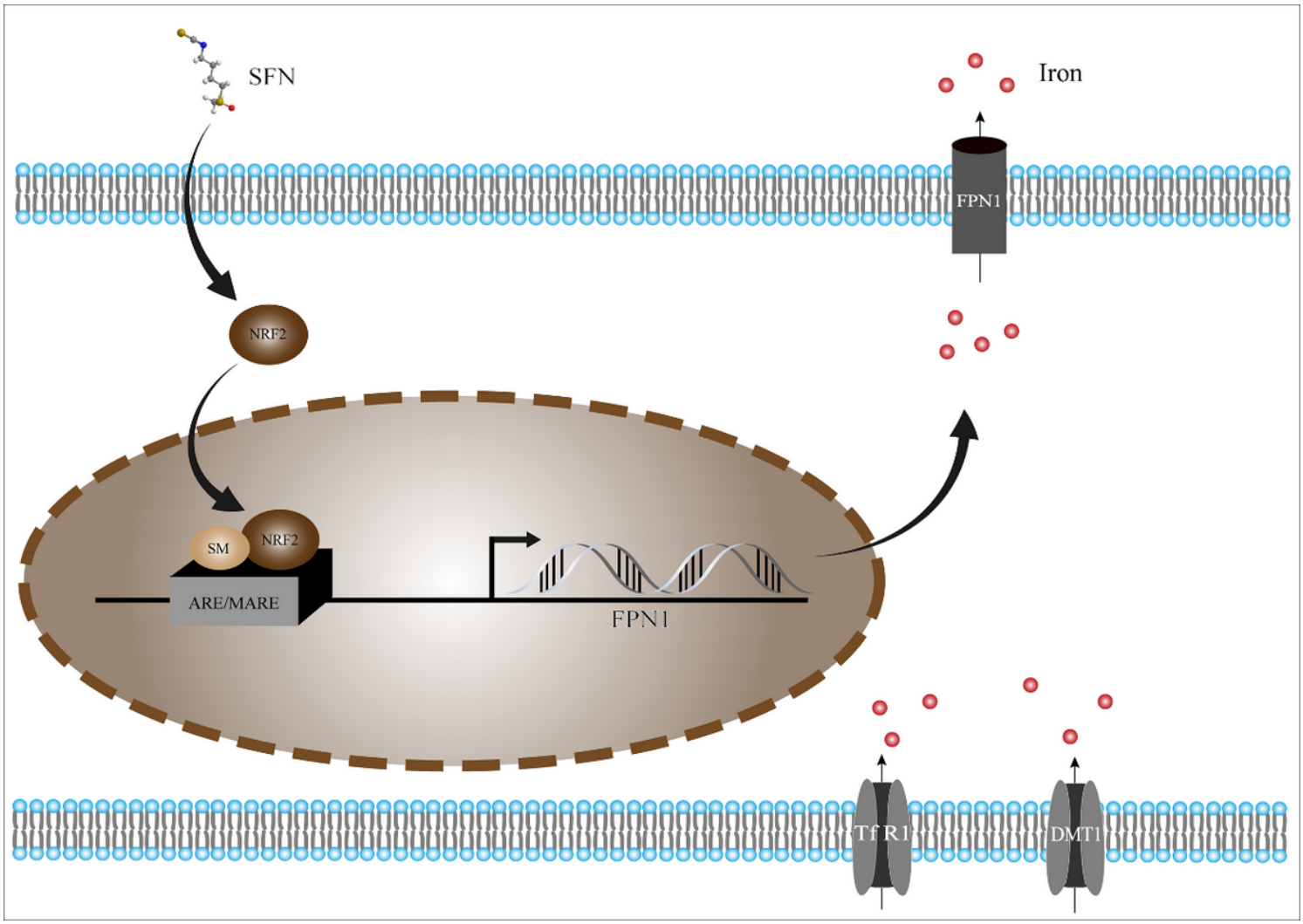


**Figure 7**

The effects of NRF2 activation on iron metabolism in cardiomyocytes. After SFN pretreatment, activated NRF2 translocates from the cytoplasm to the nucleus. Subsequently, NRF2 forming a heterodimer with small MAFs (SM) enhances the transcription of FPN1. Overloaded free iron is exported to the plasma via FPN1, which proves the protective effect of the NRF2 induction against ferroptosis.

## Supplementary Files

This is a list of supplementary files associated with this preprint. Click to download.

- Onlinefloatimage8.png